

# Adaptive Evolutionary Control for Complex Quadrotors Subject to 12-DOF Dynamic Uncertainties

Messaoud Mokhtari <sup>#1</sup>, Elham Hajeej <sup>\*2</sup>

<sup>#</sup> Department of electronics, Batna 2 University, <sup>\*</sup> Department of electronics, Batna 2 University, Laboratory LAAAS, Faculty of technology, 05000 Batna, Algeria

<sup>1</sup>m.mokhtari@univ-batna2.dz

<sup>2</sup>elham.hajeej@etu.univ-batna2.dz

**Abstract**— This paper introduces an adaptive nonlinear control architecture for quadrotor systems, where model reference adaptive control is combined with a backstepping-based design and tuned through evolutionary optimization. A twelve-degree-of-freedom dynamic model is considered, in which each state dynamic is influenced by parametric and external uncertainties. Genetic algorithms are employed to automatically refine the adaptive parameters to enhance tracking performance and reduce energy consumption. The simulation results highlight the improved stability and robustness of the optimized controller when applied to complex quadrotor maneuvers under these uncertain 12-DOF conditions.

**Keywords**— Adaptive Nonlinear Control, Evolutionary Optimization, MRAC, Backstepping, Quadrotor Dynamics

## I. INTRODUCTION

Quadrotors attract significant interest in civil and military fields thanks to their maneuverability and VTOL capability. Yet, their control remains difficult due to nonlinear dynamics, strong coupling, and sensitivity to uncertainties and disturbances [1]. These challenges intensify when translational and rotational states are affected by parametric variations and unmodeled effects.

Adaptive and intelligent approaches have been explored to address these issues. Model Reference Adaptive Control (MRAC) effectively manages uncertainties by adjusting laws in real time [2], while backstepping offers a recursive stabilization method for nonlinear systems, though often demanding in effort and tuning [3]. To enhance performance in uncertain environments, optimization tools like Genetic Algorithms (GAs) have been applied to tune parameters in backstepping and sliding mode control, reducing errors and improving robustness [4].

Most strategies, however, are used separately. This work proposes a unified framework combining MRAC and backstepping, with GA optimization of adaptive gains and control parameters. Tested on a nonlinear 12-DOF quadrotor under uncertainties and disturbances, the scheme aims to improve trajectory tracking, efficiency, and robustness in challenging flight conditions [5][6].

## II. MRAC–BACKSTEPPING CONTROL FOR A NONLINEAR QUADROTOR UNDER UNCERTAINTIES

### A. Nonlinear Quadrotor Model

The position vector  $\xi(m) \triangleq [x \ y \ z]^T \in \mathbb{R}^3$  defines the location of the quadrotor in the inertial reference frame  $R_e(O_e, x_e, y_e, z_e)$ . The body-fixed reference frame  $R_b(O_b, x_b, y_b, z_b)$ , attached to the quadrotor, is used to express the linear velocity  $[\dot{x} \ \dot{y} \ \dot{z}]^T$  and the angular velocity  $\Omega \triangleq [\Omega_1 \ \Omega_2 \ \Omega_3]^T$ , typically expressed in  $R_b$ . Each rotor  $i \in \{1, 2, 3, 4\}$  generates a thrust force  $F_i = b \omega_i^2$ , where  $b$  is the thrust coefficient and  $\omega_i$  is the rotor's angular speed. The total torque vector acting on the quadrotor, denoted  $\Gamma_b = [\Gamma_\phi \ \Gamma_\beta \ \Gamma_\psi]^T$ , is generated by the differential thrusts and rotor drag effects, and is expressed in the body frame.

Furthermore, the orientation of the quadrotor is described by the vector of Euler angles  $\eta(m) \triangleq [\varphi \ \beta \ \psi]^T \in \mathbb{R}^3$ , where  $\varphi$ ,  $\beta$ , and  $\psi$  represent the roll, pitch, and yaw angles, respectively. The weight of the quadrotor is given by  $P = mg$ , where  $m$  is the total mass and  $g$  is the gravitational acceleration.

The state vector of the system,  $X \in \mathbb{R}^{12}$ , can then be defined as:  $X = [\varphi \ \dot{\varphi} \ \beta \ \dot{\beta} \ \psi \ \dot{\psi} \ x \ \dot{x} \ y \ \dot{y} \ z \ \dot{z}]^T$  Combining the attitude angles and their angular rates with the translational positions and velocities..

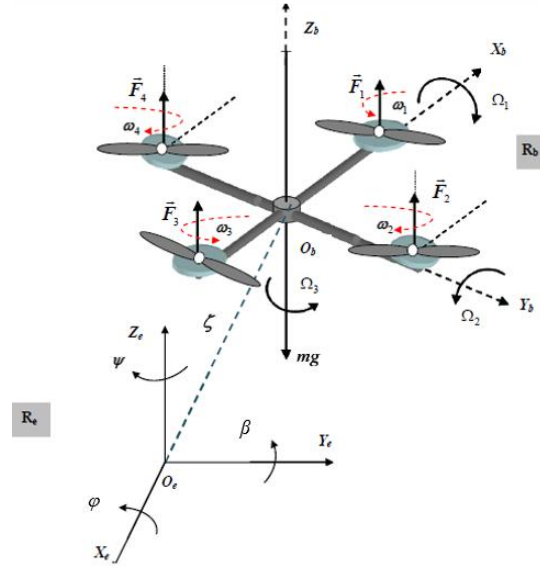


Fig. 1. Quadrotor Dynamic Geometry

In what follows, we will use the following notations for the state variables:

$$X = [x_1 \ x_2 \ x_3 \ x_4 \ x_5 \ x_6 \ x_7 \ x_8 \ x_9 \ x_{10} \ x_{11} \ x_{12}]^T \quad (1)$$

The control architecture of the quadrotor is structured around two separate control loops. The inner loop comprises four control laws:  $u_1$ ,  $u_2$ ,  $u_3$ , and  $u_4$ , responsible for managing the system's dynamic response. In parallel, the outer loop consists of two position control laws,  $u_x$  and  $u_y$ , which govern the quadrotor's motion along the  $x$  and  $y$  axes, respectively. The dynamic control variables analyzed in this study for the quadrotor are as follows:

$$u = [u_1 \ u_2 \ u_3 \ u_4 \ u_x \ u_y]^T \quad (2)$$

The control input  $u_1$  corresponds to the thrust along the body-frame  $z_b$ -axis.  $u_2$  governs the roll motion (right/left), generating the torque  $\Gamma_\varphi$ ;  $u_3$  controls the pitch motion (forward/backward), producing the torque  $\Gamma_\beta$ ; and  $u_4$  regulates the yaw rotation, resulting in the torque  $\Gamma_\psi$  [7].

The allowable input voltages applied to the four rotors and torques are defined by the following equation:

$$V_i = \frac{1}{\eta_u} \cdot \left( \frac{d\omega_i}{dt} + \mu_0 \omega_i^2 + \mu_1 \omega_i + \mu_2 \right); i=1, \dots, 4 \quad (3)$$

based on the following expressions:

$$\begin{cases} u_x = \cos x_1 \cos x_5 \sin x_3 + \sin x_1 \sin x_5 \\ u_y = \cos x_1 \sin x_3 \sin x_5 - \sin x_1 \cos x_5 \end{cases} \quad (4)$$

The quadrotor's mathematical model with uncertainties is given by the following expressions:

$$\begin{cases} \dot{x}_1 = x_2 + d_1 \\ \dot{x}_2 = a_1 x_4 x_6 + a_2 x_2^2 + a_3 \bar{\Omega}_r x_4 + b_1 u_2 + d_2 \\ \dot{x}_3 = x_4 + d_3 \\ \dot{x}_4 = a_4 x_2 x_6 + a_5 x_4^2 + a_6 \bar{\Omega}_r x_2 + b_2 u_3 + d_4 \\ \dot{x}_5 = x_6 + d_5 \\ \dot{x}_6 = a_7 x_2 x_4 + a_8 x_6^2 + b_3 u_4 + d_6 \\ \dot{x}_7 = x_8 + d_7 \\ \dot{x}_8 = a_9 x_8 + \frac{1}{m} u_x u_1 + d_8 \\ \dot{x}_9 = x_{10} + d_9 \\ \dot{x}_{10} = a_{10} x_{10} + \frac{1}{m} u_y u_1 + d_{10} \\ \dot{x}_{11} = x_{12} + d_{11} \\ \dot{x}_{12} = a_{11} x_{12} - g + \frac{\cos x_1 \cos x_3}{m} u_1 + d_{12} \end{cases} \quad (5)$$

where the parameters  $\theta$ ,  $a_i$  ( $i = 1, 2, \dots, 11$ ), and  $b_i$  ( $i = 1, 2, 3$ ) are defined by the following expressions:

$$a_1 = \frac{(I_y - I_z)}{I_x}; \quad a_2 = -\frac{K_{fax}}{I_x}; \quad a_3 = -\frac{J_r}{I_x}; \quad a_4 = \frac{(I_z - I_x)}{I_y}; \quad a_5 = -\frac{K_{fay}}{I_y}; \quad a_6 = \frac{J_r}{I_y}; \quad a_7 = \frac{(I_x - I_y)}{I_z},$$

$$a_8 = -\frac{K_{faz}}{I_z}; \quad a_9 = -\frac{K_{ftx}}{m}; \quad a_{10} = -\frac{K_{fty}}{m}; \quad a_{11} = -\frac{K_{ftz}}{m}; \quad b_1 = \frac{l}{I_x}; \quad b_2 = \frac{l}{I_y}; \quad b_3 = \frac{1}{I_z}; \quad \theta = \frac{1}{m} \quad (6)$$

Where  $I_x$ ,  $I_y$  and  $I_z$  denote the translational drag coefficients;  $K_{fax}$ ,  $K_{fay}$  and  $K_{faz}$  represent the aerodynamic friction coefficients;  $K_{ftx}$ ,  $K_{fty}$  and  $K_{ftz}$  correspond to the translational drag coefficients; and  $J_r$  is the inertia of the rotors. The yaw torque of the quadrotor, associated with the rotational speed around the vertical axis, is computed using the combined term  $\bar{\Omega}_r$ , defined as follows:

$$\bar{\Omega}_r = \omega_1 - \omega_2 + \omega_3 - \omega_4 \quad (7)$$

The control-relevant parameters of the quadrotor model are summarized in the table below:

TABLE I. QUADROTOR MODEL PARAMETERS

Symbol	Value	Symbol	Value
$m$	0.486 kg	$K_{fay}$	$5.5670 \cdot 10^{-4}$ N/rad/s
$J$	$9.806 \text{ m/s}^2$	$K_{faz}$	$6.3540 \cdot 10^{-4}$ N/rad/s
$l$	0.25 m	$K_{ftx}$	0.0320 N/m/s
$J_r$	$2.8385 \cdot 10^{-5}$ kg.m $^2$	$K_{fty}$	0.0320 N/m/s
$I_x$	0.01 kg.m $^2$	$K_{ftz}$	0.0480 N/m/s
$I_y$	0.01 kg.m $^2$	$\mu_0$	0.0122
$I_z$	0.01 kg.m $^2$	$\mu_1$	6.0612
$K_{fax}$	$5.5670 \cdot 10^{-4}$ N/rad/s	$\mu_2$	189.63
$B$	$2.9842 \cdot 10^{-5}$	$\eta_u$	280.19

### B. Altitude Control Using Non-Adaptive MRAC-Backstepping

Figure 2 illustrates a hybrid quadrotor control architecture that integrates *MRAC-Backstepping* with *GA optimization*, highlighting adaptive-optimization coordination within a hierarchical design.

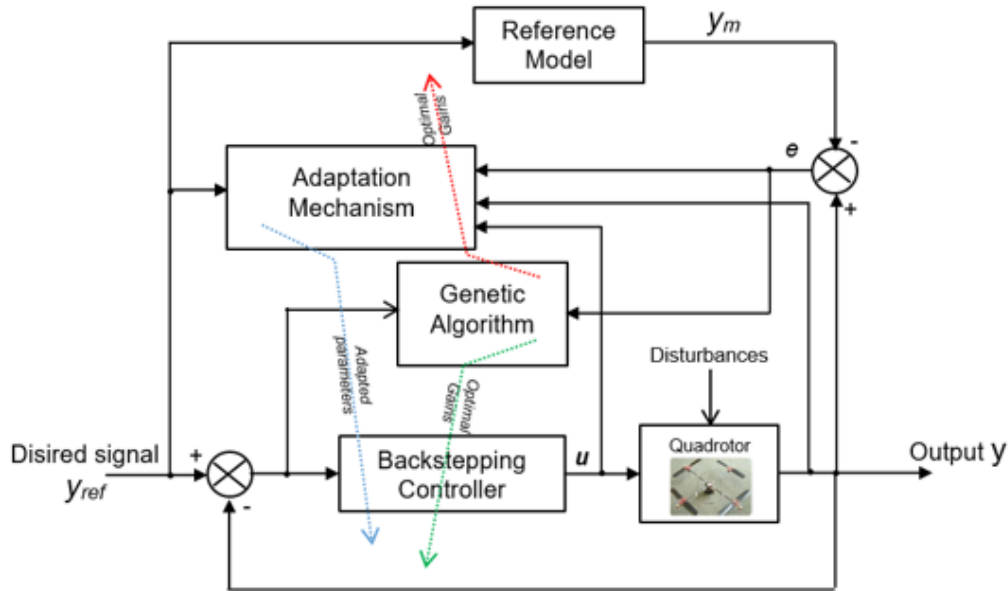


Fig. 2. Hybrid MRAC-Backstepping Control Optimized by GA for Quadrotor

The two equations considered in this study are as follows:

$$\begin{cases} \dot{x}_{11} = f(x) = x_{12} + d_{11} \\ \dot{x}_{12} = h(x) = a_{11}x_{12} - g + \frac{\cos x_1 \cos x_3}{m}u_1 + d_{12} \end{cases} \quad (8)$$

where:  $f(x)$ ,  $h(x)$  are unknown (or uncertain)

The reference model state vector is given by :

$$\begin{cases} \dot{x}_{11m} = x_{12m} \\ \dot{x}_{12m} = -2\zeta\omega_n x_{12m} - \omega_n^2 x_{11m} + \omega_n^2 z_{ref} \end{cases} \quad (9)$$

Make sure the tracking error tends asymptotically to zero, even when certain system elements are unknown.:

$$\begin{cases} e_{1z} = x_{11} - x_{11m} \\ e_{2z} = x_{12} - x_{12m} \end{cases} \quad (10)$$

Backstepping-based MRAC design starts with a systematic development of Lyapunov functions :

$$V_1 = \frac{1}{2}e_{1z}^2 \quad (11)$$

The corresponding derivative takes the form:

$$\dot{V}_1 = -k_1 e_{1z}^2 + e_{1z}(k_1 e_{1z} + x_{12} + d_{11} - x_{12m}) \quad (12)$$

Next, the virtual control  $\alpha$  for  $x_{12}$  is determined as:

$$\alpha = -k_1 e_{1z} + x_{12m} - d_{11} \quad (13)$$

The second Lyapunov function is given by:

$$V_2 = \frac{1}{2}e_{1z}^2 + \frac{1}{2}e_{2z}^2 \quad (14)$$

This leads to the following derivative:

$$\dot{V}_2 = e_{1z}\dot{e}_{1z} + e_{2z}\dot{e}_{2z} \quad (15)$$

Based on (12), (13), and (15), we can determine the control law  $u_1$ :

$$u_1 = \frac{m}{\cos x_1 \cos x_3} (-e_{1z} - k_2 e_{2z} - a_{11} x_{12} + g - d_{12} + \dot{\alpha}) \quad (16)$$

### C. Altitude Control Using Adaptive MRAC-Backstepping

To extend to the adaptive version, we will rely on the system defined in (5) and (6) and introduce the adaptation terms in the third Lyapunov function:

$$V_3 = V_1 + V_2 + \frac{1}{2\lambda_1} \tilde{a}_{11}^2 + \frac{1}{2\lambda_2} \tilde{g}^2 + \frac{1}{2\lambda_3} \tilde{\theta}^2 \quad (17)$$

which gives the corresponding derivative

$$\dot{V}_3 = e_{1z}\dot{e}_{1z} + e_{2z}\dot{e}_{2z} - \frac{1}{\lambda_1} \tilde{a}_{11} \dot{\tilde{a}}_{11} - \frac{1}{\lambda_2} \tilde{g} \dot{\tilde{g}} - \frac{1}{\lambda_3} \tilde{\theta} \dot{\tilde{\theta}} \quad (18)$$

$$\begin{aligned} &= -k_1 e_{1z}^2 - k_2 e_{2z}^2 + e_{2z} [e_{1z} + k_2 e_{2z} + \hat{a}_{11} x_{12} - \hat{g} + \hat{\theta} \cos x_1 \cos x_3 u_1 + k_1 \dot{e}_{1z} + d_{12} - \ddot{x}_{11m}] \\ &\quad + \tilde{a}_{11} \left( -\frac{1}{\lambda_1} \dot{\hat{a}}_{11} + e_{2z} x_{12} \right) + \tilde{g} \left( -\frac{1}{\lambda_2} \dot{\hat{g}} - e_{2z} \right) + \tilde{\theta} \left( -\frac{1}{\lambda_3} \dot{\hat{\theta}} + e_{2z} \cos x_1 \cos x_3 u_1 \right) \end{aligned}$$

(19)

Finally, the control law is deduced as follows:

$$u_1 = \frac{1}{\hat{\theta} \cos x_1 \cos x_3} (-e_{1z} - k_2 e_{2z} - \hat{a}_{11} x_{12} + \hat{g} - k_1 \dot{e}_{1z} - d_{12} + \ddot{x}_{11m}) \quad (20)$$

Based on (19), the adaptation laws used to update the parameter estimates are given by:

$$\dot{\hat{a}}_{11} = \lambda_1 e_{2z} x_{12}; \dot{\hat{g}} = -\lambda_2 e_{2z}; \dot{\hat{\theta}} = \lambda_3 e_{2z} \cos x_1 \cos x_3 u_1 \quad (21)$$

### III. GENETIC ALGORITHM-BASED PARAMETER ADJUSTMENT FOR BACKSTEPPING-MRAC CONTROL

In this work, a combined *Backstepping-MRAC* approach is applied to enhance stability and ensure convergence of the state error  $e_{1z}$ . The *ITAE* (Integral of Time-weighted Absolute Error) criterion guides a genetic algorithm (*GA*) to optimize controller parameters. The *GA* iteratively searches for optimal gains  $k_1$  and  $k_2$  by minimizing *ITAE*, improving error attenuation and overall stability.

The algorithm proceeds through population initialization, fitness evaluation via *ITAE*, selection, crossover, mutation, and convergence until optimal gains are found. Configured with 30 individuals over 20 generations, bounds between 0 and 0.0001, crossover probability of 0.8, and mutation rate of 0.01, the *GA* balances exploration and exploitation.

Experiments yielded a best cost value of 68.3888 compared to a mean of 68.995. By generation 20, optimized gains for altitude control were  $k_1=9.9397$  and  $k_2=9.8470$ . High gains in altitude and pitch highlight their influence, while near-zero yaw gains indicate limited contribution. In addition, the adaptation gains were identified as  $\lambda_1=1.3655 \times 10^{-5}$ ,  $\lambda_2=3.0541 \times 10^{-6}$ , and  $\lambda_3=1.4987 \times 10^{-5}$ . These optimized parameters, together with the adaptation gains, effectively reduce errors and reinforce the stability and convergence of the Backstepping-MRAC strategy.

### IV. SIMULATION RESULTS

The roll, pitch, and yaw moments were assigned values of 0.2 N·m, 0.1 N·m, and 0.05 N·m, while horizontal velocities were set to 1 m/s along the *x-axis* and 0.5 m/s along the *y-axis*. These inputs ensured stable

altitude regulation together with predefined attitude and lateral motion. The simulation results highlight the effectiveness of the integrated *MRAC-Backstepping* controller in stabilizing and guiding the quadrotor, providing accurate trajectory tracking and strong robustness. For altitude control along the *Z-axis*, the reference altitude  $Z_{ref}$  varied over time: fixed at 20 m from 0–30 s, reduced to 5 m between 30–60 s, and increased to 10 m from 60–90 s. The quadrotor parameters used in the simulation included a mass of  $m=0.486$  kg and gravitational acceleration  $g=10$  m/s<sup>2</sup>. The reference model was defined by a natural frequency  $\omega=3$  rad/s and a damping ratio  $\zeta=1$ . Figure 3 presents the genetic algorithm outcomes, showing both the best and mean fitness values.

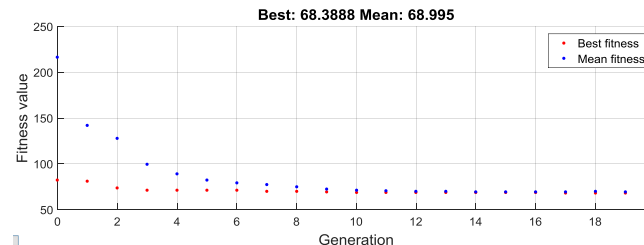


Fig. 3. Genetic algorithm results (Best and Mean fitness)

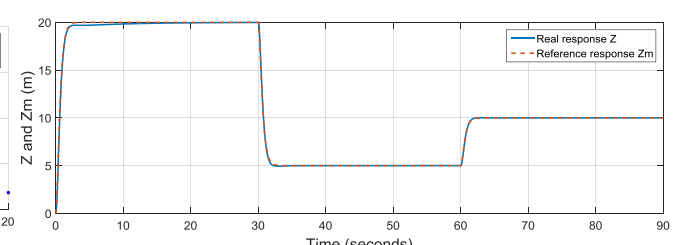
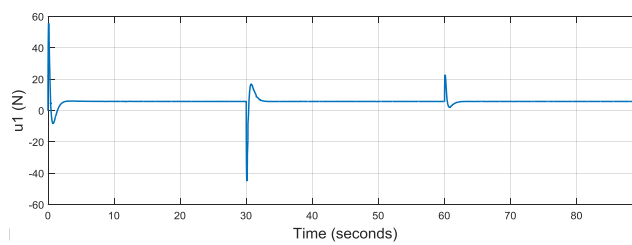
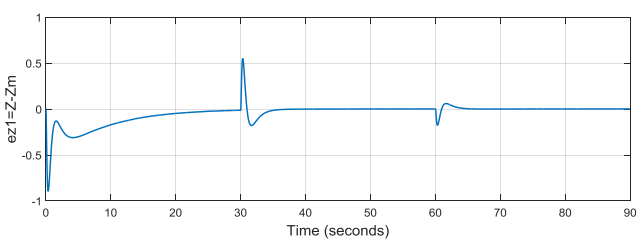
Fig. 4. Real Altitude and Reference Model Trajectory ( $z$  and  $z_m$ )

Fig. 5. Quadrotor altitude control law and Altitude Tracking Error



The simulations show accurate tracking and rapid convergence to varying setpoints, with figures confirming altitude, error, and control input, thereby validating the robustness of the proposed strategy.

The control input  $u_1$ , generated by the *MRAC-Backstepping controller*, remains smooth and bounded throughout. Signals adapt effectively to altitude and attitude changes: moderate in the first phase, increased in the second to follow dynamic references, and stabilized in the final phase. These outcomes confirm the controller's adaptability and stability under varying flight conditions.

## V. CONCLUSION

This paper proposed an integrated control strategy combining MRAC and backstepping for a nonlinear quadrotor with 12-state dynamics. A damping term was added to improve robustness and reduce effort, while a genetic algorithm optimized the control gains. The approach achieved better tracking, lower effort, and strong disturbance rejection, with simulations confirming stability and resilience under varying conditions. Future work will address real-time implementation and extension to cooperative multi-drone systems with communication delays and external disturbances.

## REFERENCES

- [1] J. Li, L. Wan, J. Li, & K. Hou, "Adaptive Backstepping Control of Quadrotor UAVs with Output Constraints and Input Saturation," *Applied Sciences* (MDPI), vol.15, no. 13, p. 8710, 2023.
- [2] A. Glushchenko, & K. Lastochkin, "Quadrotor trajectory tracking using model reference adaptive control under parametric uncertainty," *Computation*, vol. 11, no. 8, p. 163, 2023.
- [3] Shevidi, M., & Hashim, F. H., "Adaptive Backstepping and Non-Singular Sliding Mode Control for Quadrotor UAVs with Unknown Time-Varying Uncertainties," *American Control Conference (ACC)*, arXiv:2407.07175, 2024.
- [4] Y. L. Mulualem, G. G. Jin, J. Kwon, & J. Ahn, "Backstepping Sliding Mode Control of Quadrotor UAV Trajectory," *Mathematics*, vol. 19, no. 13, p. 3205, 2025.
- [5] O. Rodríguez-Abreo, J. M. García-Guendulain, R. Hernández-Alvarado, A. Flores Rangel, & C. Fuentes-Silva, "Genetic Algorithm-Based Tuning of Backstepping Controller for a Quadrotor-Type Unmanned Aerial Vehicle," *electronics*, vol.10, no. 9, p. 1735, 2020.
- [6] M. Maaruf, A. N. Abubakar, & M. M. Gulzar, "Adaptive Backstepping and Sliding Mode Control of a Quadrotor," *Springer, J. Braz. Soc. Mech. Sci. Eng.*, vol. 46, no. 630, 2024.

[7] K. Shao, W. Xia, Y. Zhu, C. Sun & Y. Liu, "Research on UAV Trajectory Tracking Control System Based on Feedback Linearization Control–Fractional Order Model Predictive Control," *Processes*, vol. 03, no. 13, p. 801, 2025.